scientific reports

Check for updates

OPEN

An amplification mechanism for weak ELF magnetic fields quantum-bio effects in cancer cells

Amirali Zandieh[1], Seyed Peyman Shariatpanahi[1]✉, Amir Abas Ravassipour[1], Javad Azadipour[1], Maryam Sadat Nezamtaheri[1], Zahra Habibi-Kelishomi[1], Mojtaba Ghanizadeh[1], Ali Same-Majandeh[1], Keivan Majidzadeh-A[2], Amir Taheri[3], Alireza Madjid Ansari[3], Mohammad Amin Javidi[3], Mohammad Mehdi Pirnia[1] & Bahram Goliaei[1]✉

Observing quantum mechanical characteristics in biological processes is a surprising and important discovery. One example, which is gaining more experimental evidence and practical applications, is the effect of weak magnetic fields with extremely low frequencies on cells, especially cancerous ones. In this study, we use a mathematical model of ROS dynamics in cancer cells to show how ROS oscillatory patterns can act as a resonator to amplify the small effects of the magnetic fields on the radical pair dynamics in mitochondrial Complex III. We suggest such a resonator can act in two modes for distinct states in cancer cells: (1) cells at the edge of mitochondrial oscillation and (2) cells with local oscillatory patches. When exposed to magnetic fields, the first group exhibits high-amplitude oscillations, while the second group synchronizes to reach a whole-cell oscillation. Both types of amplification are frequency-dependent in the range of hertz and sub-hertz. We use UV radiation as a positive control to observe the two states of cells in DU and HELA cell lines. Application of magnetic fields shows frequency-dependent results on both the ROS and mitochondrial potential which agree with the model for both type of cells. We also observe the oscillatory behavior in the time-lapse fluorescence microscopy for 0.02 and 0.04 Hz magnetic fields. Finally, we investigate the dependence of the results on the field strength and propose a quantum spin-forbidden mechanism for the effect of magnetic fields on superoxide production in Q_o site of mitochondrial Complex III.

Since the early observations concerning effects of the alternating weak magnetic field with frequencies below 3 kHz on living organisms[1–3], there have been ongoing efforts to explain how interactions with energy dozens of magnitudes below k_BT are not being masked by thermal noise. In a constant low-intensity magnetic field, the energy of the interaction with electron magnetic moments is many orders of magnitude less than the thermal fluctuation. It is also the case for a quantum of energy in an AC field in this range of frequencies. The fact that Extremely Low-Frequency Magnetic Fields (ELF-MF) are too weak to act on chemical reactions in biological systems is commonly referred to as the "kT Problem" in the literature[4,5].

In this regard, the most widely discussed mechanism was proposed based on the notion that the chemical reactions which involve free radicals can be strongly influenced by static magnetic fields and is commonly designated as Radical Pair Mechanism (RPM)[6,7]. In brief, if a chemical bond with an opposite spin paired electron is broken, the subsequent recombination of resulting free radicals is only possible if the two electrons preserve their total spin angular momentum and stay in the singlet state. The effect of a nearby source of magnetic field like nuclear magnetic moment can cause interconversion from singlet to triplet states, which has been experimentally detected recently[8]. Two out of the three triplet states with non-zero spin component (T_{+1} and T_{-1}) can be energetically affected by an external magnetic field and this, depending upon details of the particular molecular structure and strength of the field, which can alter the transition rate of singlet–triplet conversion[9]. Based on this mechanism Ritz et al. proposed an interesting explanation for Wiltschkos' observation in the 1970s concerning a possible magnetic compass in European robins[10,11].

[1]Institute of Biochemistry and Biophysics, University of Tehran, Tehran, Iran. [2]Genetics Department, Breast Cancer Research Center, Motamed Cancer Institute, ACECR, Tehran, Iran. [3]Integrative Oncology Department, Breast Cancer Research Center, Motamed Cancer Institute, ACECR, Tehran, Iran. ✉email: pshariatpanahi@ut.ac.ir; goliaei@ut.ac.ir

Observations for the effect of weak-magnetic fields have gone beyond the scope of a specific cell-line or phenomenon. This could open an exciting realm regarding the effect of these fields on all cells which may be promising for medical applications.

A growing number of studies are indicating the effect of static and ELF magnetic fields on the level of apoptosis in normal and cancer cells[12,13]. On the other hand, the cellular level of Reactive Oxygen Species (ROS), as a major component in cellular signaling pathways and particularly apoptosis, has been frequently reported to be affected by ELF exposure[14–17]. Thus, a possible link between ROS and magnetic fields effects via an RPM scheme seems reasonable. Recently, Kinsey et al. suggested a possible radical pair mechanism to explain their observation on modulation of superoxide by weak magnetic field in which the field could inhibit or increase the stem cells proliferative response following injury in an intensity-dependent manner[18].

Electron transfer chain (ETC), in the inner membrane of mitochondria, and more precisely complex I and III are the main sites of superoxide production[19]. It is also the primary source of ROS and involves in many vital processes in the cell[20]. Observations suggest several components of these electron transporters as the primary target of magnetic fields for their effects on ROS level and mitochondrial inner membrane potential[21–23]. Further, evidence of a promising candidate for the RPM in ETC is experimentally observed in complex III[24]. Complex III (aka cytochrome bc1) is an essential component in respiratory and photosynthetic ETC which oxidize quinol and reduce one-electron redox carriers in a process known as "Q Cycle" and generates an electrochemical gradient of protons that ultimately drives the synthesis of ATP. In the initial step of the cycle, at a site called Q_o, a single electron transfer to the "Rieske" FeS cluster of the complex produces a free radical semiquinone (SQ) intermediate[25]. Although the exact sequence of electron and proton transfers at this site is mostly debated, the "leakage" of an electron from the main route to the adjacent oxygen molecules is generally considered as the main mechanism of superoxide production. In 2013, Sarewicz et al. reported a semiquinone at the Q_o site (SQ) that is coupled to the reduced Rieske cluster (FeS) via spin–spin exchange interaction detected by transitions in EPR spectra[24]. More recently the same group reported a metastable triplet state for SQ which is non-reactive with oxygen that presents a gated mechanism at Q_o site[26]. This electron pair can be an interesting candidate for the mentioned radical pair mechanism.

Physiological effects of such RPM call for a drastic change of intracellular ROS concentration through an amplification mechanism. Attempts to introduce such amplification mechanism is not unprecedented in the literature. Eichwald and Walleczek suggested a general amplification scheme for RPM amplification based on enzyme kinetics[27,28] and Katting et al. proposed a weak magnetic field amplification in flavin-containing radical pairs through slow radical termination reactions[29]. More recently, Player et al. employed the Brusselator model oscillator to present a amplification mechanism for amplitude of limit cycle oscillations in the concentrations of reaction intermediates[30].

In addition, the mentioned amplification mechanism should be capable of explaining frequency dependency of the observed phenomena in order of few hertz as it is frequently reported in experiments[31–35]. Our recent study reported different windows of effective frequencies for observed response including elevated intracellular ROS level, morphological changes, and cell death in different cell lines[36]. Given the fact that the frequency of the only oscillatory step in the original RPM scheme ($S\text{-}T_0$ interconversion) is on the order of tens of megahertz[37], observations in the range of few hertz indicate a non-trivial underlying amplification mechanism.

Periodic cell-wide depolarizations of mitochondrial membrane potential (Ψ_m) which are triggered by reactive oxygen species (ROS) and propagated by ROS-induced ROS release (RIRR) have been postulated to contribute to cardiac arrhythmogenesis and injury during ischemia/reperfusion[38]. Two different modes of RIRR have been described: Ψ_m oscillations involving ROS-sensitive mitochondrial inner membrane anion channels (IMAC), and slow depolarization waves related to mitochondrial permeability transition pore (MPTP) opening[39].

Under normal conditions, mitochondrial respiration is accompanied by low-level ROS production neutralized by powerful antioxidant systems. During metabolic stresses (e.g., ischemia and reperfusion), however, ROS levels can increase, which in turn can trigger additional ROS production and release from the mitochondria. Aon et al. showed that locally generated ROS can trigger cell-wide Ψ_m oscillations and fast propagating waves[40]. They proposed IMAC-mediated RIRR to explain cell-wide oscillations and waves observed in their experiments, from which Cortassa et al. developed a mathematical model incorporating the sensitivity of IMAC to superoxide anion (O_2^-) in the intermembrane space[41].

ROS play an important role in tumorigenesis and affect multiple biological processes such as cell proliferation, genomic instability, inflammation, resistance to apoptosis and metabolic reprogramming. Indeed, increased levels of ROS are observed in a number of cancer cell lines and mitochondrial superoxide flash in tumor cells has been confirmed experimentally[42]. Kuznetsov et.al clearly showed RIRR in four different cancerous cell-line and, more importantly, oscillation of Ψ_m and mitochondrial ROS release by laser-induced oxidative stress in these cells[43]. A key observation has recently suggested that the induction of ROS pathways by laser-induced singlet oxygen generation can trigger oscillation of mitochondrial membrane potential in a melanoma cell line and not in the normal one[44]. We suggest a mechanism by which cancer cells avoid cell-wide oscillation and its probable consequences like apoptosis. Further, we illustrate how it can be a key to explain the effect of extremely-low frequency magnetic field on cancer cells via an amplification phenomenon.

Built upon a model previously developed for the simulation of the observed oscillation of ROS level in myocytes[45], we show how the pictured alteration in superoxide production can escalate the whole cellular ROS level via two different modes: [I] Triggering oscillation for the cells with borderline level of superoxide production that avoid oscillation altogether, and [II] Synchronizing out of phase oscillatory mitochondria via a resonance phenomenon for the cells which scape whole mitochondrial network synchronization by reaching high frequency oscillations. Overall, the model describes how the minor changes caused by RPM can be amplified and affect the organism at cellular level. Moreover, it explains the dependency of the bio-effect on the

frequency of applied magnetic fields in the order of few Hertz frequency which, to the best of our knowledge, has not been addressed in previous studies.

In addition, we experimentally observed the effect of fields at the order of 10 to 100 millitesla on intramitochondrial ROS level and mitochondrial membrane potential and demonstrated the frequency dependence of these effects. Also, here we used UV radiation, which was previously shown to trigger elevation of superoxide production[46], as a positive control to characterize our cell lines mitochondrial network behavior in the absence of magnetic fields. Finally, we will delineate a radical pair-based scheme for the quantum-bio effects of weak magnetic fields on Complex III in mitochondria.

In a nutshell, our proposed scheme acts in two distinct levels: [I] At the level of superoxide production in mitochondrial ETC where the applied magnetic field can alter production rate of superoxide by closing the energy gap between singlet and triplet state of a radical pair in Complex III. Here the applied magnetic field effectively act as static field. And [II] at the level of mitochondrial network, where oscillation of the applied magnetic field (and thus oscillation in the production rate of superoxide) can resonate with the intrinsic frequency of RIRR in cancer cells. At this level, the minor effect of underlying RPM is amplified to affect the physiology of the cell in a frequency-dependent manner.

Methods

Reaction–diffusion model for mitochondrial network

Here we developed our model based on the Yang et al. PDE model for Cardiac Myocytes. The two-dimensional mitochondrial network consisting of 25×5 coupled voxels with each unit containing a three-compartment single mitochondria model: mitochondrial matrix, intermembrane space, and cytosol.

The full description of the model and the equations can be found in the supplement.

Modelling the effect of external magnetic field

The major component and fluxes of the model in each single mitochondrion unit are shown in Fig. 1.

Based on Sarewicz et al. findings[24], we assume that superoxide production V_s depends on the leakage of electron from Complex III of ETC (k_{shunt}) which can be affected by an external magnetic field (B_{AC}):

$$V_S = k_{shunt}(1 + B_{AC}) \tag{1}$$

And B_{AC} is defined as:

$$B_{AC} = k_B \cos(\omega t) \tag{2}$$

where t and ω are time and angular frequency, respectively, and k_B is the dimensionless amplitude. Our detailed proposal for the RPM, resulting in the ROS production rate alteration (B_{AC}), is discussed in the discussion.

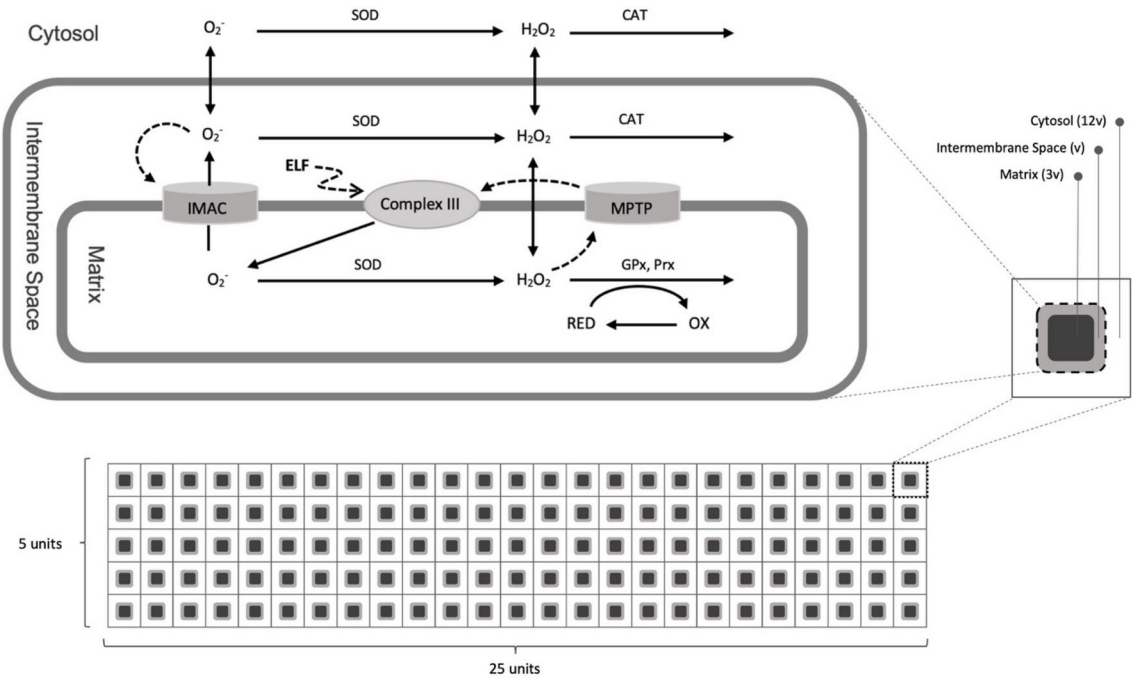

Fig. 1. The three-compartment model for a single mitochondrion unit (top) in the network. A lattice of 5×25 units (bottom) illustrates the mitochondrial network.

The produced superoxide is either dismutated into hydrogen peroxide in mitochondrial matrix or released to the intermembrane space via IMAC channels where it can inter the cytosolic space by crossing the outer membrane. The rate of superoxide release through IMAC is a function of intermembrane superoxide concentration which can potentially cause the system to show oscillatory behavior in certain sets of parameters. The production of hydrogen peroxide, which can freely cross the both inner and outer membrane, happens with higher rates of dismutation in intermembrane and cytosolic spaces compared to matrix. The resulting H_2O_2 is subsequently converted into water by glutathione peroxidase, peroxiredoxin and catalase. Finally, the MPTP channel whose opening is assumed to be a function of hydrogen peroxide concentration in matrix, can cause elevated level of superoxide production. The opening of both channels leads to the depolarization of the inner mitochondrial membrane.

The dynamic of the cytosolic ROS is investigated through the parameter space for: (1) the percentage of the electron shunt onto oxygen in complex III (aka superoxide production), and (2) the leakage of superoxide from mitochondrial matrix into the intermembrane space which is inspected for the range of 10^{-4} to 10^{4} for maximum conductance of IMAC channels. To ensure that the initial phase of each mitochondrion is independent from the rest of the system, for every simulation, superoxide production of each unit is set to start at a random time point (from a uniform distribution) during the first period of potential oscillation. The initial superoxide and H_2O_2 concentration are set to be equal for all the units in all systems. The term for the magnetic field is applied only after the system reached an equilibrium for the concentrations of both species.

Cells preparation

We used three cell lines, MDA-MB231, DU-145 and Hela purchased from the National Cell Bank of Iran (Pasture Institute, Iran). The cells were cultured and prepared as explained in the supplementary. Then cells were stained with DCFH-DA and TMRE for fluorescence microscopy of ROS and mitochondrial potential, respectively. The details are mentioned in the supplementary.

UV exposure conditions

Eight thousand cells were seeded in each well of a 96-well plate and a 20 mW, 280 nm UV LED lamp was positioned above it at a distance of 14.35 mm as illustrated in Fig. 2.

The cells were exposed to UV radiation for 30 and 60 s, and images were taken after each exposure. Control groups were incubated for the same durations as the exposed samples and captured images following each incubation. The whole setup is placed on the stage of the 405-M Zeiss microscope and the temperature is fixed at 37 °C. The details of time lapse imaging are reported in the supplementary.

Magnetic field exposed cells microscopy

A single well of a 96-well plate was separated to be placed within a magnetic circuit. The magnetic circuit consists of a 1000 turns of a 0.3 mm diameter lacquered wire coil and a U-shaped iron core with a 2 cm air gap where the well is placed (see Fig. 3).

A sinusoidal magnetic field is applied and the frequency/amplitude of the field are varied for different series of experiments. The intensity and frequency of the applied fields were in the ranges of 0 to 100 mT and 0.01 Hz to 5 Hz, respectively. Adequate heat conductivity provided and the temperature in the chambers were monitored to remain within the 0.1 degree of 37 °C during the magnetic field applications. The details of time lapse imaging are mentioned in the supplementary. Figure 3 is a schematic of the instruments that were used.

Results and discussion

The model reveals two resonance modes for the field's effect

We examined the effects of the two main uncertain parameters of the system on the oscillatory behavior of the mitochondrial network model. The first parameter examined is the percentage of electrons shunted to oxygen from Complex III (k_{shunt} in the equations), that indicates the source of superoxide production in mitochondria. Dependent on the physiological state of a cell line, the value can be in the range of one percent in normal cells up to 20 percent of the oxygen consumption in cancer cells[47].

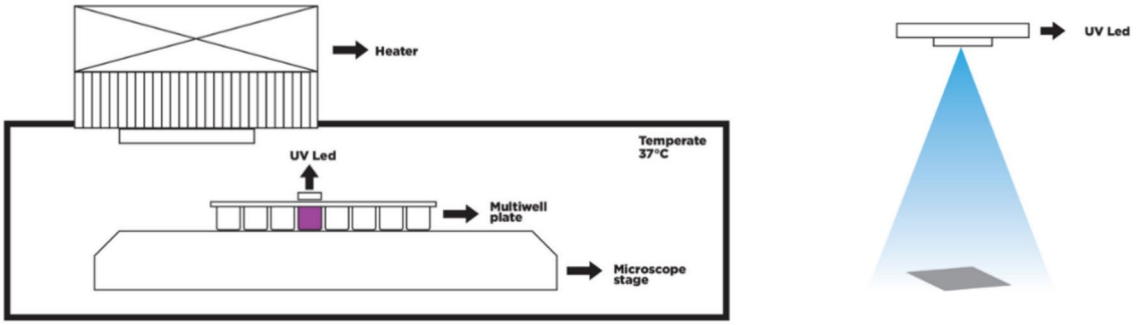

Fig. 2. Setup for fluorescent microscopy of a 96-well plate under the emission of UV.

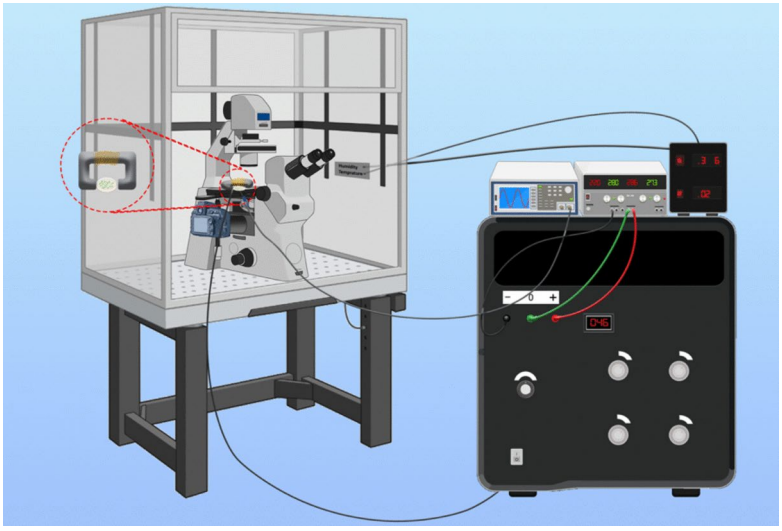

Fig. 3. A schematic overview of the devices for real-time fluorescent microscopy of cells under the exposure of the alternating magnetic field.

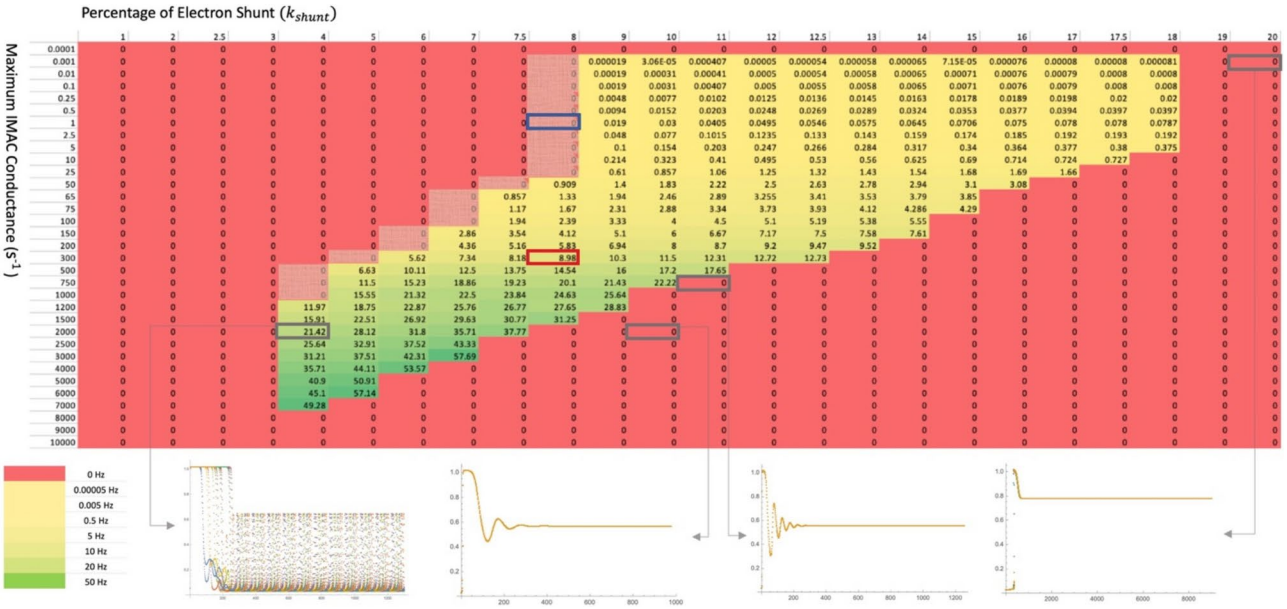

Fig. 4. Frequencies of mitochondrial oscillation for systems with different values of percentage superoxide shunt and maximum superoxide conductance through IMAC channels. Zero values indicate no oscillation. The bottom plots show the dynamic of an IMAC open probability for the cell with the set of parameters highlighted.

The second parameter is the maximum conductance of superoxide through the IMAC channels from mitochondrial matrix into the intermembrane space which is estimated to be 0.5 s^{-1} for a normal cell. This can also mirror the number of these channels on the mitochondrial inner membrane.

As depicted in the parameters phase space in the Fig. 4, for certain range of superoxide production and conductance, an oscillatory release of superoxide from matrix to intermembrane space is predicted by the model (The number in each cell indicates the frequency of oscillation). No oscillation is resulted for the cells with zero value; depending on the set of parameters, either the IMAC channels are completely closed or, in the cases with high maximum IMAC conductance, the IMAC opening probability converges to a value between 0 and 1 and the oscillation vanishes.

There are some border points (hatched cells) in which a slight change superoxide production may potentially trigger the oscillatory behavior. Here we checked this possibility by applying an alternating magnetic field which can alter the superoxide production rate in a sinusoidal manner as described in the Eqs. (1) and (2).

A set of parameters in the border region was selected (the cell with blue border in Fig. 4) and the frequency of the applied magnetic field was chosen by extrapolating the frequency value of intrinsic ROS oscillation of neighboring cells. An eight-fold increase in the cytosolic ROS peak concentration is observed when a whole cell oscillation triggered by applying a 0.01 Hz alternating magnetic field. Next, a range of frequencies and intensities of the applied magnetic field were tested to investigate their effects on triggering the oscillatory behavior (the same set of parameters i.e. the cell with blue border). The parameter k_B, which determines the maximum change in superoxide production, is utilized to set the intensity of the field. The results can be found in Fig. 5. The applied magnetic field with matching frequency of system has to affect the superoxide yield by at least 0.5 percent to trigger the network oscillation. This value is generally higher for frequencies other than the intrinsic frequency except in the cases where frequency is an integer multiple of the original frequency (see frequency 0.02 Hz in the figure).

As the second mode of resonance, alternating magnetic field can also affect the oscillatory state of the network by synchronizing the already existing out of phase oscillations. Independent oscillatory patches of mitochondria can be observed in systems with relatively high frequencies in our simulations. Figure 6 illustrates time series map of superoxide concentration in the 2D network model during two periods of oscillations (the 1st and 2nd row in the figure). The oscillatory patches can be detected as clusters of mitochondrial units with synchronous elevation of cytosolic superoxide concentration.

For different sets of parameters, the portion of the repeated experiments in which unsynchronized oscillation are observed vary from few percent up to the all simulations. To check if these out of phase patches can be synched, under the effect of an external magnetic field, a set of parameters in which all the repeated simulations

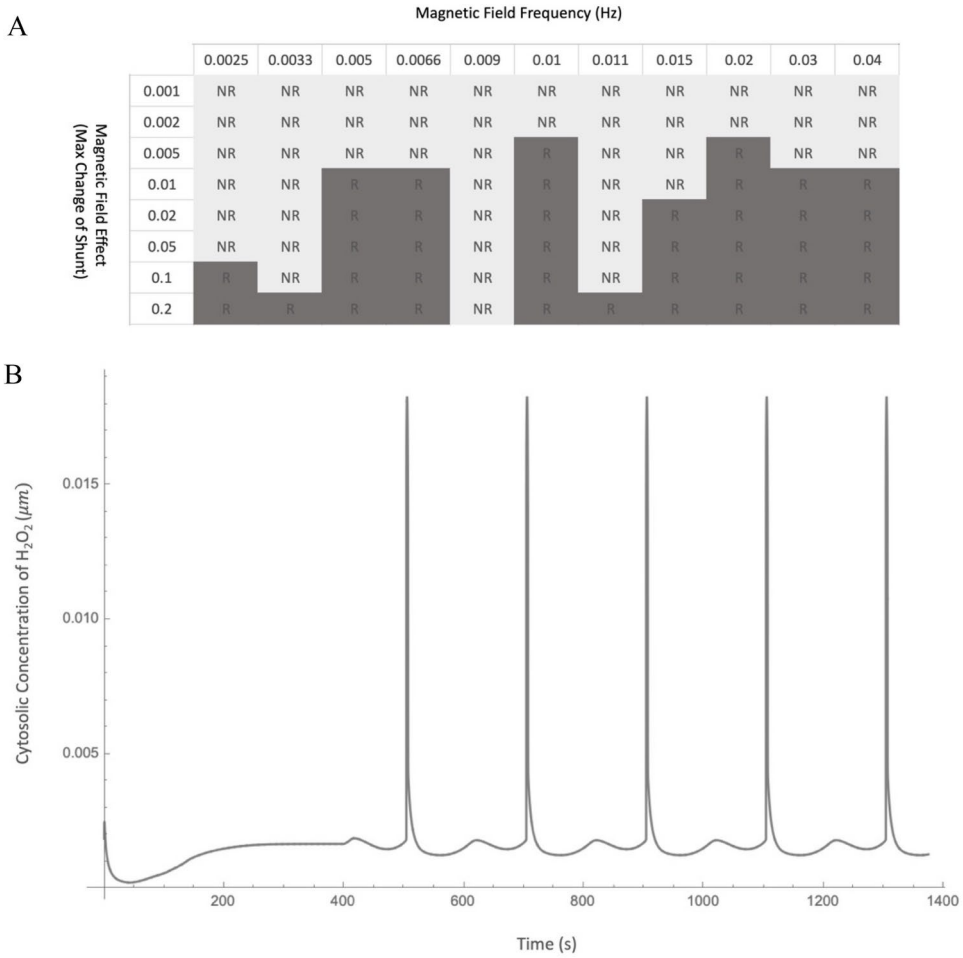

Fig. 5. (**A**) Effect of Frequency and Intensity of the applied magnetic field on triggering mitochondrial oscillation in the border systems. Simulations were performed for shunt = 8 and $k_{IMAC} = 1\ s^{-1}$ where a frequency of 0.01 Hz was obtained by extrapolating the frequency values of neighboring cells. Dark gray (R) cells indicate triggered oscillation while the light gray cells (NR) denote that the applied field failed to induce whole cell oscillation. (**B**) The oscillation of cytosolic concentration of H_2O_2 when a 10 percent fluctuation in superoxide production by a 0.01 Hz magnetic field is applied. Magnetic field is applied from 400 s. The vertical axis indicates the spatial average of H_2O_2 concentration throughout the cytosolic units in the system. About 8 folds increase in maximum level of cytosolic H_2O_2 can be observed compared to the baseline concentration (1.84×10^{-3} to 2.54×10^{-4} M).

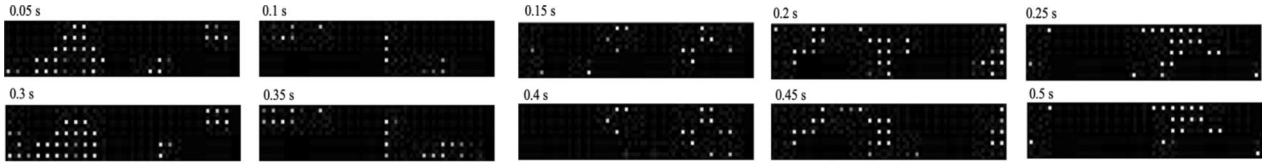

Fig. 6. Time series depiction of superoxide concentration in each unit of the mitochondrial network model. Several patches of mitochondria with simultaneous release of superoxide into the cytosol are evident. The first and the second rows show two successive periods of the oscillation. The brightness of each white dot corresponds to the IMAC open probability of its respective mitochondrion which correlates with the superoxide efflux into the intermembrane space.

resulted in out of phase oscillatory patched is selected (The cell with red border in Fig. 4, $shunt = 8$ and $k_{IMAC} = 300\ s^{-1}$). Again, ranges of frequencies and intensities are tested and the results can be found in Fig. 7. The number in each cell indicates the fraction of simulations in which the whole cell was synchronized by applying field with the corresponding frequency and intensity. Likewise, minimum change of superoxide production by field for synchronization of the system is observed to be 0.5 percent of yield. However, depending on phase and arrangement of the synchronous patches, this phenomenon does not necessarily happen in all the simulations repeats. By raising the field intensity, the whole network synchronization is guaranteed to happen for certain frequencies (cells with the values equal to 1 in Fig. 7A).

Both modes of alternating magnetic field effect, triggering cell-wide oscillation and synchronizing out of phase oscillators, show frequency and intensity dependence. Both effects result in higher intermembrane and cytosolic concentrations of superoxide and thus peroxide at their peak levels which can potentially open the mitochondrial permeability transitions pores (MPTP) on the mitochondrial inner membrane[48]. It was also shown experimentally that the opening of MPTP by ELF exposure is mediated by ROS[49]. This is a crucial and mostly irreversible step in triggering the apoptosis process. Thus, this is conceivable that despite the necessity of higher concentrations of ROS in cancer progression, tumor cells avoid cell-wide oscillation of mitochondrial network. In our model, this is possible either by avoiding oscillatory state of single mitochondrion altogether or via maintaining the conditions with unsynchronized oscillatory patches of mitochondria, which is feasible in higher frequencies.

There is a third way for a tumor cell to avoid a whole-cell RIRR altogether. Cancer cells have been shown to have fragmented mitochondrial network. It is becoming increasingly clear that mitochondrial fission enhances the proliferation and metastasis of cancer cells[50,51]. This type of morphology for the network is reflected in the lattice structure of our model where disconnected mitochondria are only linked through diffusion of species in the cytosol. However, if a cancer cell can somehow adopt to have a connected network structure, it might help mitochondria to avoid RIRR and, consequently, the effects alternating magnetic fields. In fact, this might be even another reason that normal cells with balanced fission/fusion dynamics are not affected by such fields. Testing this hypothesis through our model confirms that more connected morphologies tend to show oscillatory behavior in a narrower range of parameters. We simulate three other network structures other than the original model to account for the more connected topologies (Fig. 8). Generally, the oscillation of RIRR was observed for a smaller range of superoxide production rates and IMAC channels conductance compared to the fragmented topology (Fig. 8A). In the extreme case, where all the mitochondria are completely connected (Fig. 8D), no oscillatory behavior is detected for the inspected range of parameters. In this scenario, the alternating magnetic field is unable to exert any amplification effect through either of the introduced modes. Note that we did not account for the higher rate of superoxide production generally reported in the more fragmented networks like cancer cells[52]. Including this factor rationally can add to observed trend in our simulation. A broader range of structures and more extensive investigation of parameters may be needed to reach a definitive conclusion.

UV induces rapid mitochondrial membrane depolarization

To investigate our hypotheses on normal and induced synchronized dynamics of the mitochondrial states in cancer cells, we performed time lapsed fluorescence microscopy.

The variations were both observable in UV-exposed and control samples across cells, but the UV exposed samples contained more cases with excited mitochondrial networks.

We observed fairly rapid flashes of TMRE signals (a mitochondrial inner membrane potential indicator) when applying UV on our examined cell lines. These flashes are mostly characterized by sudden change of signal intensity in subcellular compartments. Also, whole-cell increase and subsequent decrease of the TMRE emission are evident in some of the UV exposed cells (see videos in the supplementary). A sudden shift in the intensity of a compartment in cell may be the result of the of the mitochondrial network synchronization.

Interestingly, besides whole cell synchronization of the mitochondrial network within a single cell, an inter-cellular synchronization of the networks of neighboring cells can also be observed which is probably mediated by H_2O_2 among cells. The lower panel of Fig. 9 suggests a propagation of H_2O_2 signal from Cell 3 to Cell 1 and Cell 2 which are in comparable distance from Cell 3. The latter two cells show a similar pattern of TMRE flashes with alike time delays from the source signal.

The observations indicate probable excitability of mitochondrial networks in our investigated cell line, similar to what previously proposed for myocytes during ischemic-reperfusion injury[38]. Also, the data shows a steeper drop in signal intensity of UV-exposed cells compared to the control group. This may correlate with the Sharpe et

A

Magnetic Field Effect (Max Change of Shunt)	Magnetic Field Frequency (Hz)										
	2.245	2.99	4.49	5.99	8.08	8.98	9.88	13.47	17.96	26.74	35.92
0.001	0	0	0	0	0	0	0	0	0	0	0
0.002	0	0	0	0	0	0.1	0	0	0.2	0	0
0.005	0	0	0.2	0	0	0.4	0	0	0.5	0.2	0.1
0.01	0	0	0.4	0	0.2	0.8	0.2	0	0.6	0.3	0.1
0.02	0	0	0.5	0	0.2	0.8	0.2	0.2	0.6	0.5	0.2
0.05	0	0	0.7	0.1	0.6	1	0.5	0.3	0.7	0.5	0.6
0.1	0.2	0	0.7	0.2	0.6	1	0.9	0.3	1	0.8	0.9
0.2	0.4	0	1	0.5	1	1	0.8	0.6	1	1	1

B

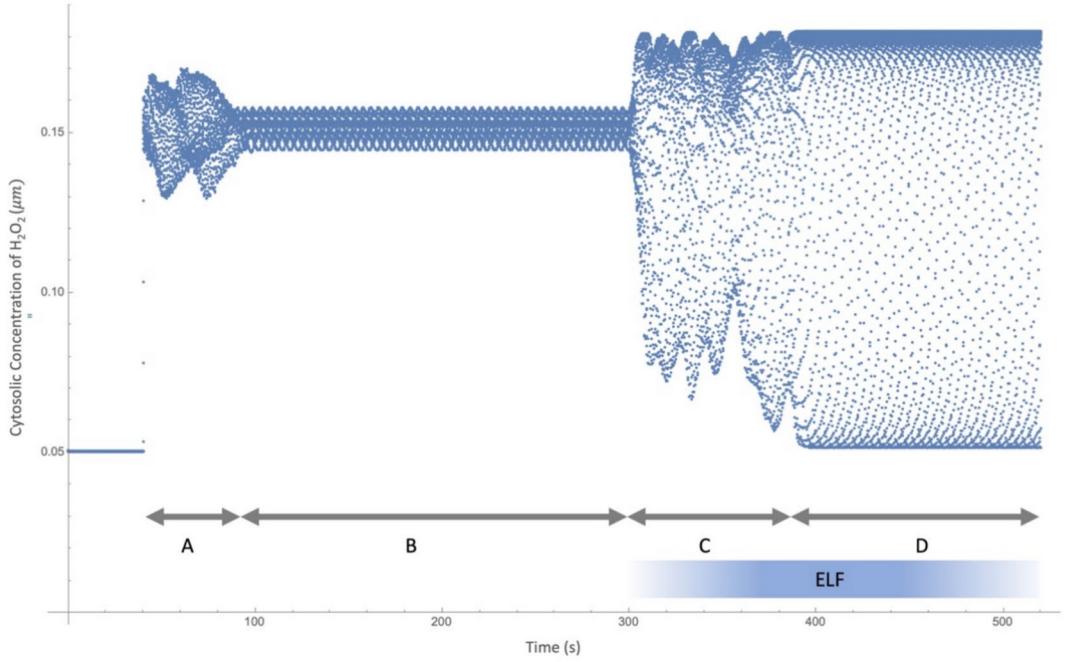

C

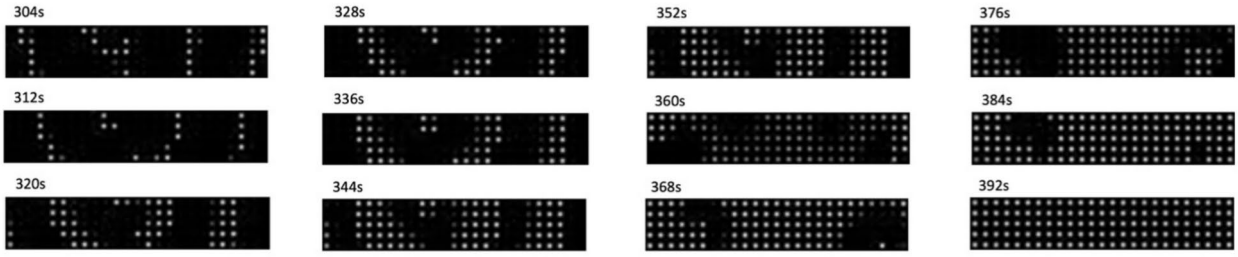

Fig. 7. Synchronization of mitochondrial oscillatory patches under the effect of magnetic field. (**A**) Effect of Frequency and Intensity of applied magnetic field on synchronization of mitochondrial oscillation in the network. Numbers in the cells indicate the proportion of synchronized network out of 10 simulations. Simulations were performed for shunt = 8 and $k_{IMAC} = 300\ s^{-1}$ where an unsynchronized oscillation with intrinsic Frequency of 8.98 Hz was observed (cell with red border in Fig. 4). (**B**) The dynamic of cytosolic H_2O_2 concentration (averaged over all cytosolic units in the system) when a 10 percent fluctuation of superoxide production under 8.98 Hz magnetic field is applied. After several asynchronous periods of oscillations (part A), a number of synchronous patches of mitochondria emerges in the network (part B). By applying the oscillatory magnetic field, the patches start to merge into a synchronized oscillatory unit (part C) until the whole network reaches a fully synchronized state (part D). The apparently convoluted diagram in the figure is due to the two very different dynamic time scales of oscillations and synchronization states. (**C**) Time series depiction of superoxide concentration in each unit of the mitochondrial network model under the effect of alternating magnetic field. An 8.98 Hz magnetic field is synchronizing the out of patches of oscillatory mitochondria progressively.

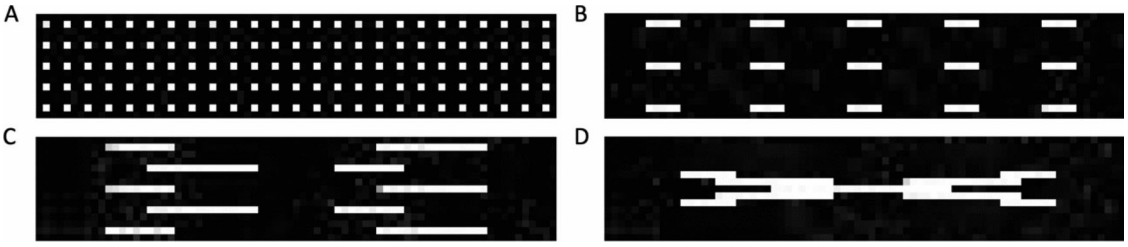

Fig. 8. Different simulated topologies of the model with varying levels of connectedness in the mitochondrial network. White cells represent the mitochondrial matrix, while black cells represent either the mitochondrial intermembrane space or cytosol. All structures have the same average mitochondrial density across the whole cell.

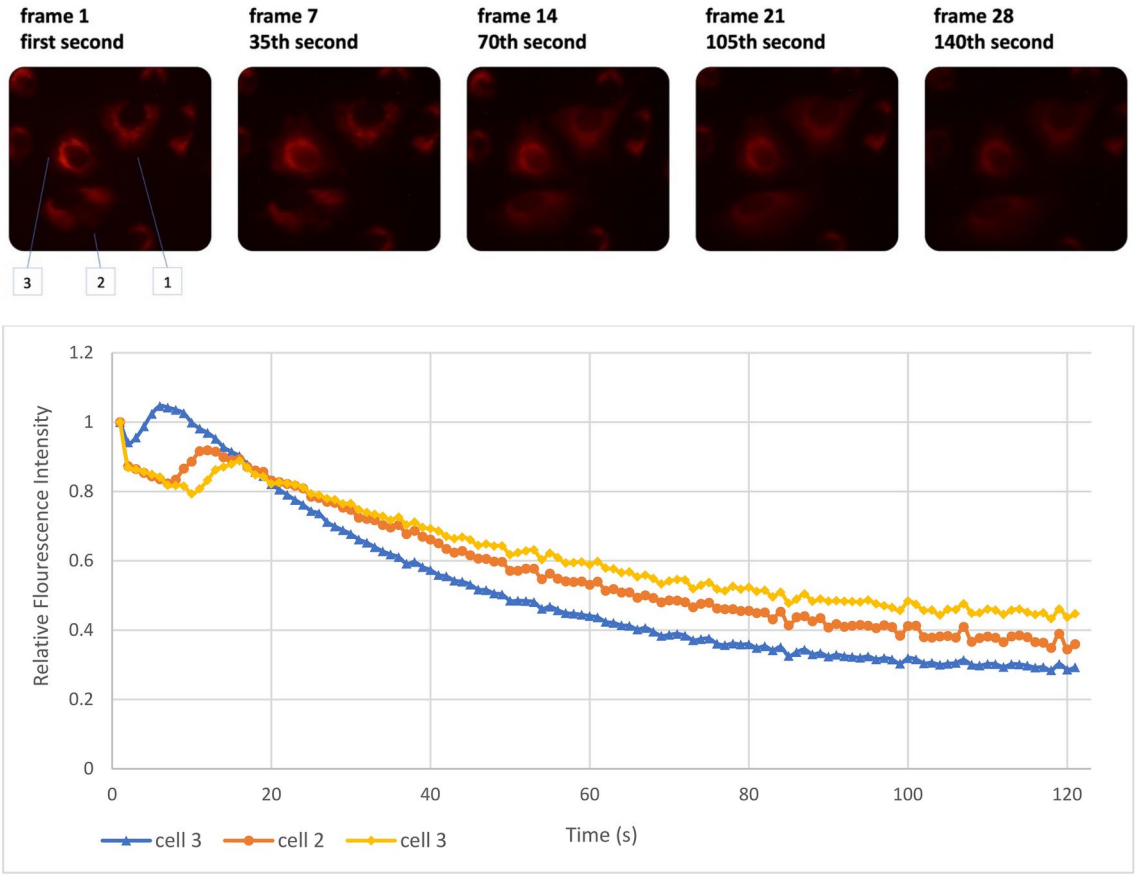

Fig. 9. Three cases of transient increase in TMRE emission for the UV treated cells of DU cell-line. The upper panel depicts an increase in signal in the second picture (second 35) (see videos in the supplementary). The same is evident in the lower panel in which an elevated signal emission in one of the cells is followed by same phenomenon for the other two adjacent cells.

al. observation on glioblastoma in which a rotating magnetic field induce mitochondrial permeability transition (MPT, reported the based on the attenuation of TMRE signal) and transient increase in ROS production[53]. In compliance with their report, an increase in ROS production can also trigger MPTP and loss of mitochondrial membrane potential (and thus TMRE signal) in our model.

Furthermore, simultaneous change in signal intensity of two different compartment of Cell 2 (Fig. 9) may indicate the patch organization of mitochondrial network, as described in the model. In such a case, the mitochondrial network of cell 2 is comprised of two synchronous patches with opposite phase of oscillation (as illustrated in Fig. 9).

Mitochondrial membrane potential of DU and Hela show different responses to UV exposure

A dual response is observed for DU and Hela cell lines after a 60 s exposure to UV irradiation. Level of TMRE emission decreased during the 10 min observation for both cell lines. The transient elevation of signal in exposed DU cells is the product of rapid hyperpolarization and subsequent depolarization of mitochondrial membrane of the cases noted in previous section (Fig. 9). However, in contrast to Hela, the pace of mitochondrial membrane potential loss is significantly higher for DU cells compared to its control group (Fig. 10). This may imply the role of UV exposure in pushing DU cells beyond required ROS level for oscillatory threshold which leads to opening of IMAC and loss of electric potential in inner mitochondrial membrane. In contrast, Hela cells possibly behave according to the second mode of our model prediction, where the open state of mentioned channels are already present for a cell with asynchronous oscillatory mitochondrial network. Thus, even if the synchronization of oscillatory mitochondria is reached in such a cell line, a difference between the rate of depolarization (i.e. TMRE signal attenuation) for the test and the control group is not expected.

Higher levels of ROS in Hela cells generate more DCF radicals which in turn can produce more superoxide via reaction with oxygen[54]. This along with photo-reactivity of DCFH[55] can explain the increasing trend of fluorescence emission for these cells. The UV exposure augments ROS production and the subsequent phenomena which is evident in the test group of Hela cells (Fig. 11). These processes are also present in DU cells, though less-pronounced. Thus, the diminishing effect of DCFH diffusion out of cells dominates the dynamics of emission after an initial increase via the aforementioned processes. Hence, the downward trend of DCFH emission is preceded by a rising episode in the control group. This increasing part is not present in the UV exposed group which is probably due to the fact that the imaging was not started until after the 60 s of UV application. This delay prior to imaging was necessary to avoid unintended excitation of the dye by UV.

Magnetic fields induce frequency dependent mitochondrial membrane depolarization

The emitted signal of TMRE and DCFH are recorded for five cell-lines (DU, MDA, Hela, MC4L2, and SkBr3) under the effect of alternating magnetic field and also the controls groups. Compared to control groups, the rate of signal reduction was observed to be significantly higher for the field-treated cells of DU, MDA, and MC4L2. This rate was observed to be in the same range in control and test groups of Hela cells. Compared to the other cell lines, SkBr3 shows insignificant rate of signal attenuation. This rate is one and two order of magnitude below other observation for DCFH and TMRM, respectively (Note the scale of the vertical axis). Figure 11A shows a rapid drop of TMRE signal intensity for a selected single cell compared to an untreated cell in three different frequencies. This indicates a fast depolarization of mitochondrial inner-membrane electric potential.

As can be seen in Fig. 12A,C,G, compared to the majority of the tested frequencies, the average rate of TMRE signal attenuation for all cells is negligible for the control groups of DU, MDA, and MC4L2 cells (Although less pronounced in the later case). Further, this rate significantly differs between the tested frequencies in all cases which indicates a frequency-dependent effect in the observations. Stronger effects are seen in lower frequencies for DU and a sharp drop is evident for 0.1 Hz for MD, and MC4L2 cells which can reflect a more pronounced resonance effect. In the case of Hela, the differences are either not significant or less conclusive compared to other cell lines. These results are in agreement with UV experiments. The table of resulted p-values for t tests between all the group pairs are available in the supplement.

The drops in TMRE signals are possibly due to opening of IMAC channels based on the first mode of field action in our model (triggering oscillation in border states). The different results for magnetic field frequency (see Fig. 2S of the supplementary) can be attributed to various intrinsic frequencies of affected mitochondria

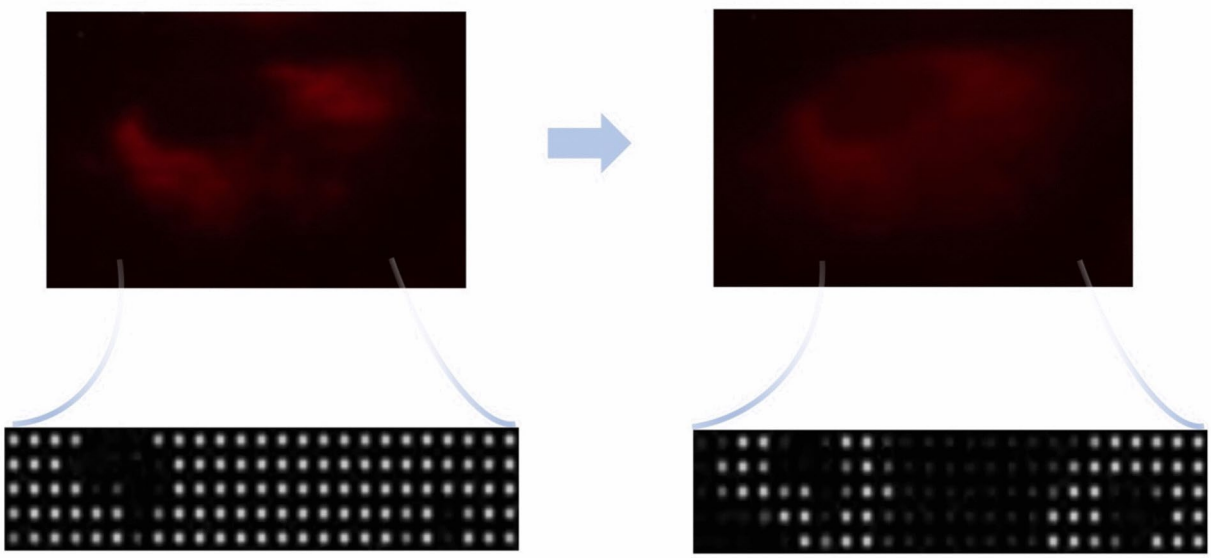

Fig. 10. Sudden change in signal intensity of TMRE in certain parts of a cell may indicate patchy structure of mitochondrial network oscillation.

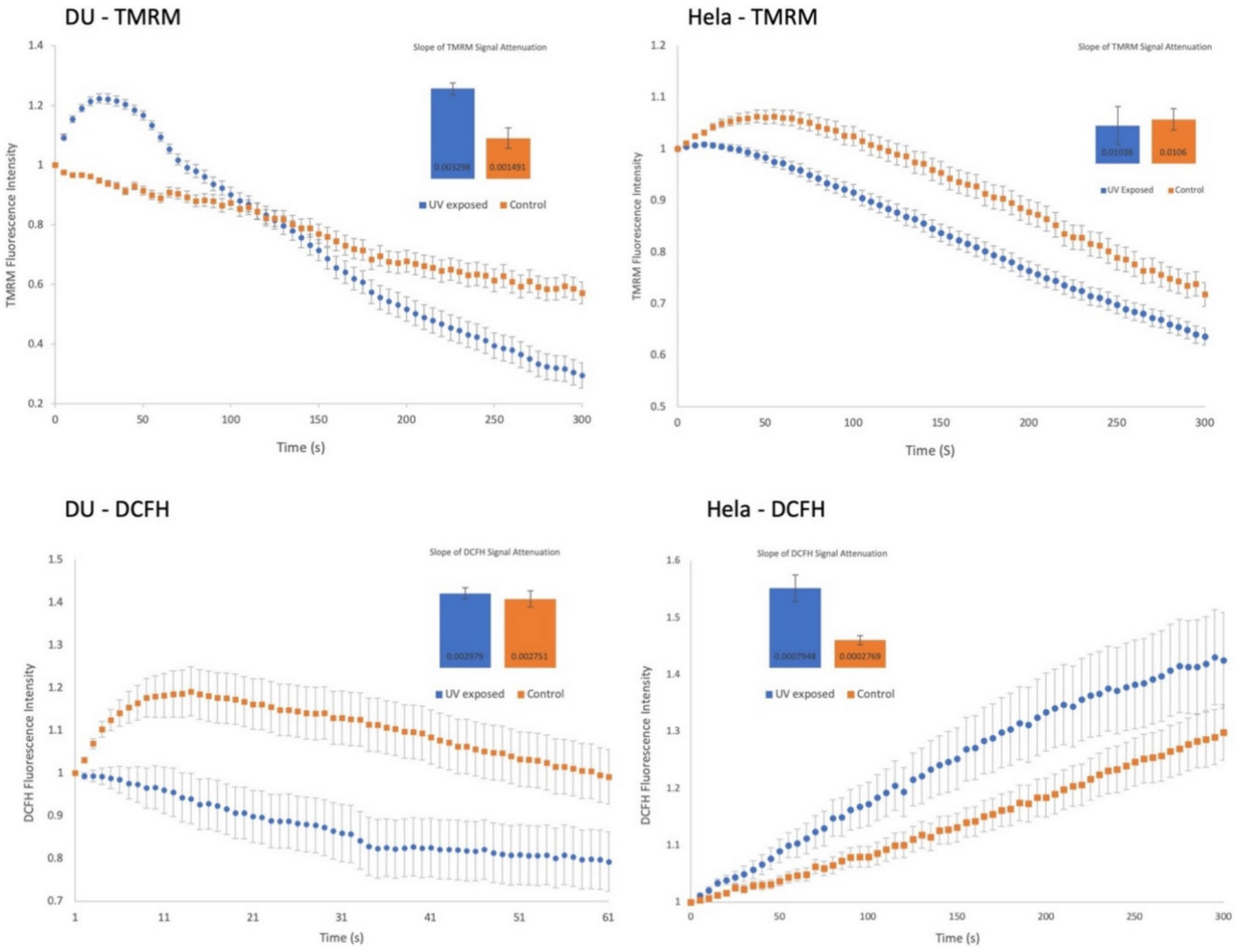

Fig. 11. Fluorescence intensity of TMRE (upper plots) and DCFH (lower plots) for DU and Hela after a 60s UV exposure. Slope of signal reduction is shown for each plot.

which resonate with the applied magnetic field. In contrast, the rapid fall of this signal for both field affected and control group in Hela cells (Fig. 12E) can be explained by our second mode of action for the magnetic field in our model: for a cell with already oscillatory mitochondria, though unsynchronized throughout the network, a synchronizing magnetic field is not expected to gravely affect the overall trend of signal attenuation. Figure 12G shows four instances of TMRM fluorescence intensity of single DU cells exposed to magnetic field with different frequencies.

Similar drops in DCFH emission signals for DU, MDA and MC4L2 cells is observed (Figs. 11D,H, 12B), which is expected to correlate with their intracellular ROS concentration. This result, which is also observed in UV tests for DU (Fig. 11A), may be explained by higher rate of ROS scavenging in cytosol as the result of synchronized release of superoxide from the mitochondrial network into the cytosol[56]. Overall increase of this signal for control groups of all three cell lines during the observation is likely due to the photo-oxidation of DCFH molecules which usually occur in high level of this dye (Fig. 12B,D,F)[55]. Moreover, spontaneous reaction of DCF radical with the oxygen in such concentration can add to this phenomenon[54]. Steeper increase in DCFH emission of control group for Hela cells due to the higher concentration of ROS is anticipated based on our UV tests. In this case, dynamic of DCFH emission in the field-treated Hela cells show marked difference compared to the control group. This may be due to the synchronization of already oscillating patches of mitochondria of these cells which results in strong whole cell oscillation that encompass all the mitochondria, even those were probably not oscillating before. Contrary to UV exposed Hela cells which irradiation adds up to their high level of superoxide production, application of magnetic field did not amplify the DCFH signal in Hela cells. In fact, here the synchronization leads to a more effective dismutation of cytosolic superoxide and thus no significance overall increase can be seen.

Lin et al. reported a significantly more connected mitochondrial network structure for SkBr3 cells compared to the MDA using dynamic light scattering microscopy[57]. As described above, cells with interconnected network topology are expected to show oscillatory RIRR in a more limited set of parameters or not exhibit oscillations altogether (Fig. 8). Consequently, we suggest that SKBr3 cells lack the prerequisites needed for the amplification effect of magnetic fields. This is reflected in insignificant effects of applied magnetic field compared to other

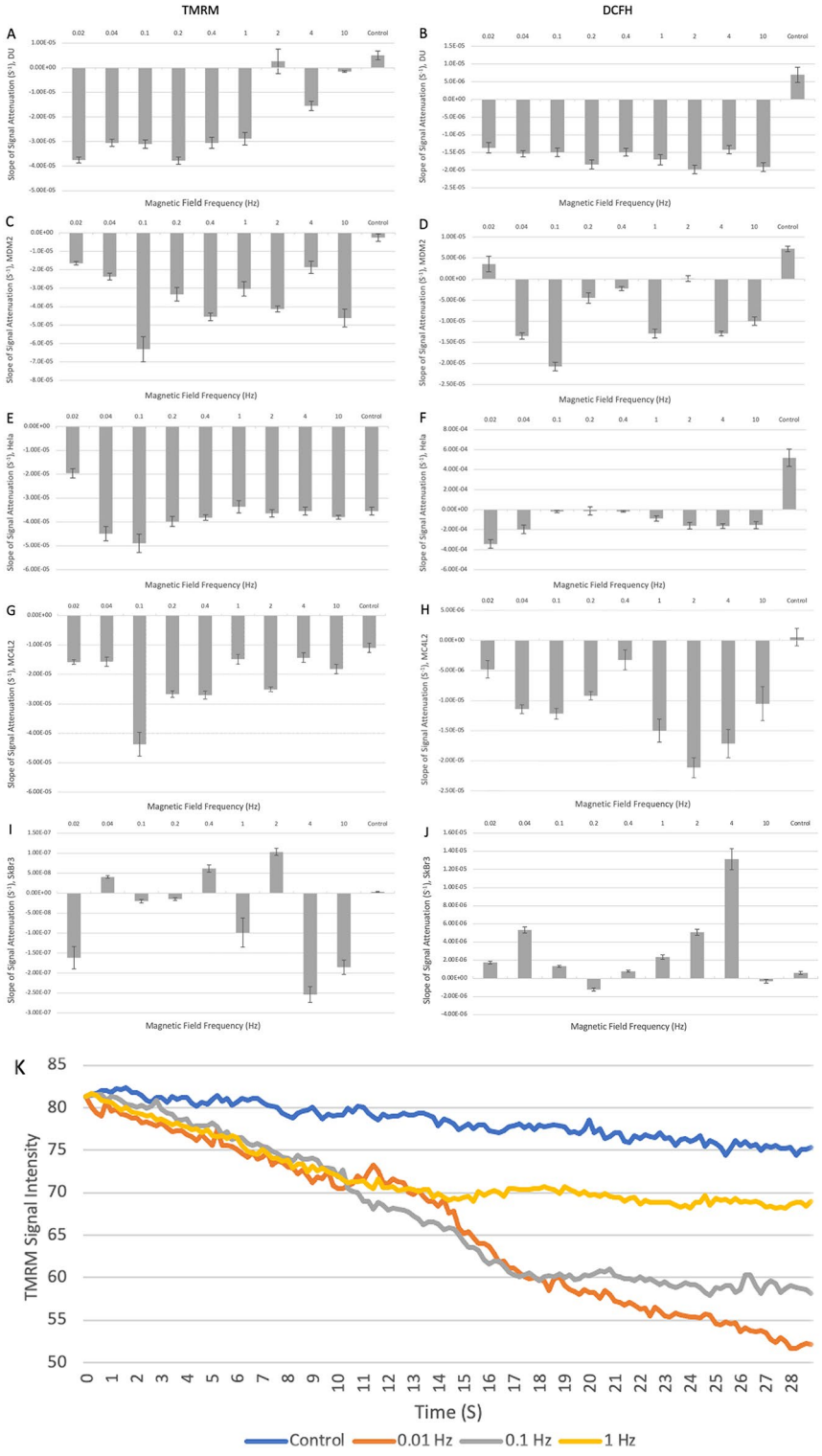

Fig. 12. (**A**–**J**) The rows illustrate the rate of signal attenuation of TMRE and DCFH emissions for DU, MDA, Hela, MC4L2 and SkBr3 cell line, respectively. The rates were averaged for 70 randomly selected cells for each experiment. (**G**) Fluorescence intensity for four DU cells exposed to magnetic field with different frequencies. Each series indicate a single cell.

cell lines in our experiments (Fig. 12I,J). This unresponsiveness can also arise due to the fact that the cells with interconnected mitochondrial network tend to produce less superoxide overall[52].

Mitochondrial membrane potential and ROS level oscillates with the frequency of the applied field

As a sign of triggering oscillations, several instances of oscillatory dynamics of mitochondrial inner membrane potential and whole-cell ROS level are detected in our observations for lower frequencies. The frequency of the fluctuations matches with that of the applied magnetic field despite overall diminishing trend of TMRE and DCFH signal intensity. Figure 13A illustrates three periods of oscillation in the average signal intensity of 70 DU cells under the effect of 0.02 Hz magnetic field. Five cycles of oscillation within a 124-s period are evident in the average DCFH signal of MC4L2 cells exposed to a 0.04 Hz magnetic field which correspond to a matching frequency (Fig. 13B).

Triggering oscillatory behavior in mitochondrial network is in line with our proposed idea of resonance between varying magnetic field and a system of coupled mitochondria with the same intrinsic frequency. The similar frequencies of applied field and fluorescent signals indicates border state of the treated cell population.

Effect of field intensity on signal attenuation

Attenuation of TMRE signal is measured for all three cell lines in different intensities of magnetic field (10, 20, 50 and 100 mT). The applied frequency for each cell line was selected to maximize the observed effect (see Fig. 12B). The optimal frequency was 0.1 Hz for Hela and MDA and 0.02 Hz for DU. The results show a more rapid signal exhaustion in higher intensities of magnetic field (see Fig. 14). Again, the control group for the Hela cells show

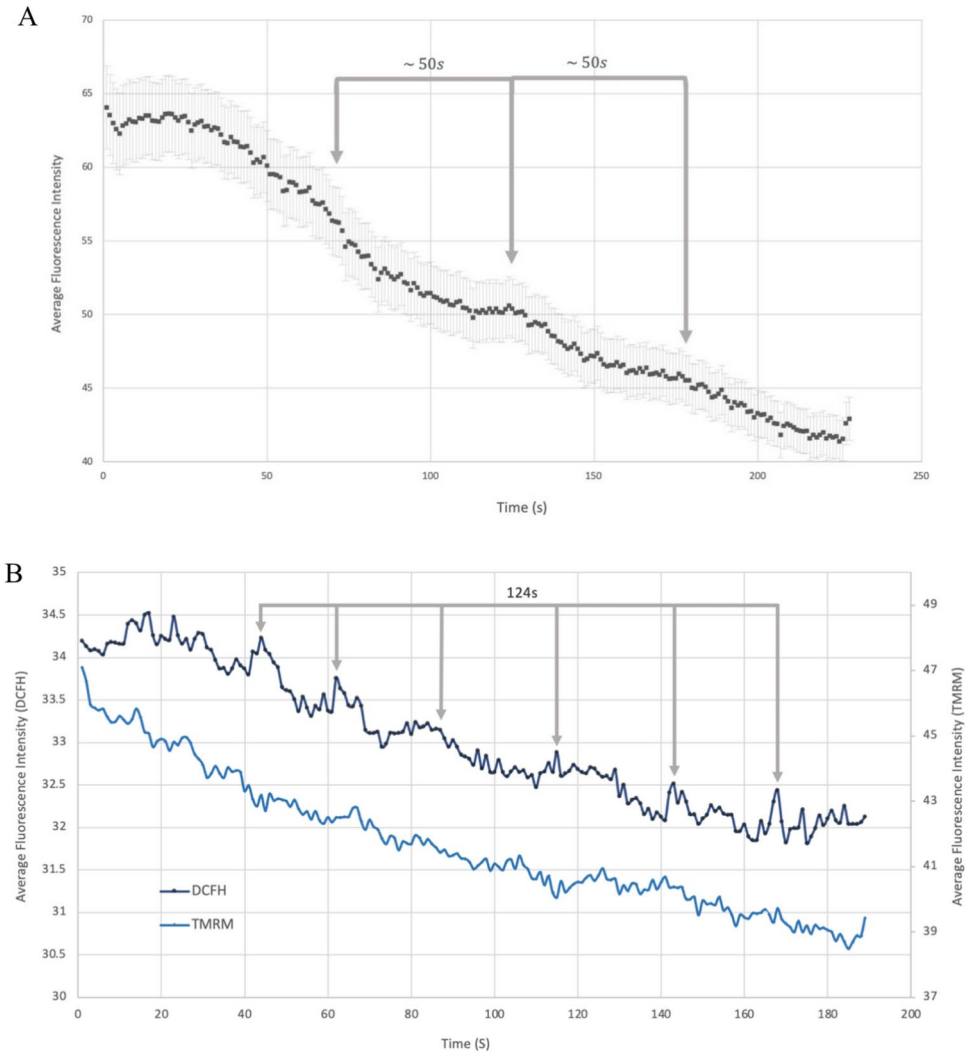

Fig. 13. Oscillatory behavior of fluorescent signals. (**A**) Average TMRM signal of intensity of DU cells (number of cells: 70) under the effect of alternating magnetic field (0.02 Hz and 100 mT). Three periods of oscillation are apparent in the plot (roughly 50 s/0.02 Hz). (**B**) Average signal intensity of TMRM and DCFH for 70 randomly selected MC4L2 cells exposed to a 0.04 Hz alternating magnetic field.

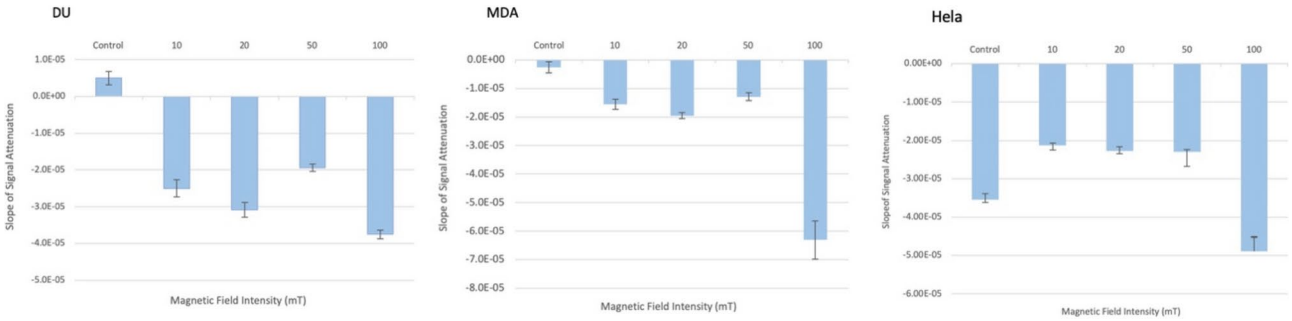

Fig. 14. Slope of TMRE attenuation for two cell lines while exposed to the magnetic fields with different field intensities. The frequencies are 0.01 Hz for DU and 0.05 Hz for MDA and Hela cells. The table of p-values resulted from t tests for each pair of groups (control and tested intensities) are available in supplementary.

significant drop in fluorescence intensity compared to other cell lines which indicates the existence of ion efflux into mitochondrial intermembrane space even without the present of synchronizing magnetic field.

These results suggest a scheme based on the conventional radical pair mechanism in which a field intensity in the order of several hundreds of millitesla can close the energy gap between triplet and singlet state of an electron pair. Thus, a sub-100 millitesla magnetic field only partially narrows the energy interval of the states. As discussed later, this energy gap is in agreement with Sarewicz et al. findings where the spin–spin exchange interaction value, found in Cytochrome bc1 Complex, is estimated to be a few gigahertz[24].

Usselman et al. proposed a superoxide and flavin based radical pair for explain the change in ROS level in rat pulmonary atrial muscle cells and human umbilical vein endothelial cells under the effect oscillating magnetic field[58,59]. More recently, Zadeh-Haghighi has also suggested a similar scheme for magnetic field effect on planarian regeneration where they mentioned Complex I of ETC as the possible site of superoxide-flavin radical pair formation[60]. However, superoxide has exceedingly fast spin relaxation of superoxide due its symmetry (few nanoseconds[61]) which cause the coherent time of such a radical pair to be few orders shorter than the required effective time for magnetic fields in their suggested models. Beutner et al. have recently reported the effect of a static low-intensity magnetic field on several component of ETC and suggest a RPM as the possible mechanism[62]. Here we propose a novel scheme based on the conventional radical pair mechanism that suggests how applying low-intensity magnetic field can change the level of triplet species of SQ–FeS and subsequently affect superoxide production rate in Q_o site of the Cytochrome bc1 Complex.

Figure 15 is a simplified diagram of different stages of electron transfer from quinol to either heme b_L or O_2 in complex III based on Sarewicz et al. scheme[26]. In the first step (V_T) an electron transfer from quinol to FeS generates a singlet radical pair (2) which is normally undergone a subsequent electron transfer to reduce heme b_L (7 via V_F) but also can dissipate (6 via V_D), interconvert into a triplet state (4 via ISC), shunt an electron onto an O_2 to form a superoxide (8 via V_s), or form a hydrogen bond with histidine (3). Forming a hydrogen bond is a key event in Sarewicz et al. scheme since it forms metastable states (3 and 4) which are non-reactive with O_2 and thus act as protection buffer which prevent superoxide production. In fact, the triplet state is only detected in the metastable form since in the normal process, fast rate of semiquinone oxidation ($V_F \approx 10^9\ s^{-1}$)[63] prevents significant triplet formation or advancing in any of the other mentioned paths. In case of impeded forward reaction, slow spin relaxation of iron-sulfur[64] allow a coherent intersystem crossing for accumulated (unbounded) singlet radical pair which generates a detectable signal of triplet species.

Sarewicz et al. calculated a J = 3500 MHz for energy gap between singlet and triplet species with hydrogen bond which clearly prevent any interconversion by hyperfine coupling (2J in Fig. 15). Since the initial radical pair forms in the singlet state, assuming an approximate rate of $\approx 108\ s^{-1}$ for hydrogen bond formation, it is conceivable that the bonded triplet and singlet are in strong disequilibrium. Thus, we suggest that a magnetic field with a corresponding singlet–triplet interconversion frequency of 3500 MHz (roughly equal to 125 mT) can increase the relative abundance of the triplet to singlet pool which can alter superoxide production as discussed below. This is in line with the findings of Yamashita and Saito, who reported an increase in cell respiration by a factor of 1.3 upon exposure to a magnetic field with similar order of intensity[65].

Details of superoxide production as a result of charge transfer from semiquinone (V_S in Fig. 15) was studied by Salo et al.[66]. Though they only consider the singlet state of SQ–FeS radical pair in this process, charge transfers from triplet states are also plausible. In this scheme, one of the cases of electron transfers from triplet SQ–FeS to the adjacent molecular oxygen can be characterized as a spin-forbidden reaction (Fig. 16A). Electrons can shift onto the nearby Oxygen molecule only when its unpaired electrons have an anti-parallel spin alignment relative to the radical pair (Fig. 16B). Thus, elevated level of triplet to singlet species ratio under the effect of weak external field can change the rate of superoxide production.

Although the current study explored the mechanistic aspects of the observed phenomena, it did not directly address the therapeutic potential of the applied magnetic fields. However, the differential effects of these fields on tumor versus normal cells suggest their potential as a promising tool for cancer treatment. Notably, the applied magnetic fields were well below the ICNIRP-recommended maximum exposure level of 400 millitesla for static magnetic fields[67]. While this suggests no significant off-target effects under the tested conditions, we

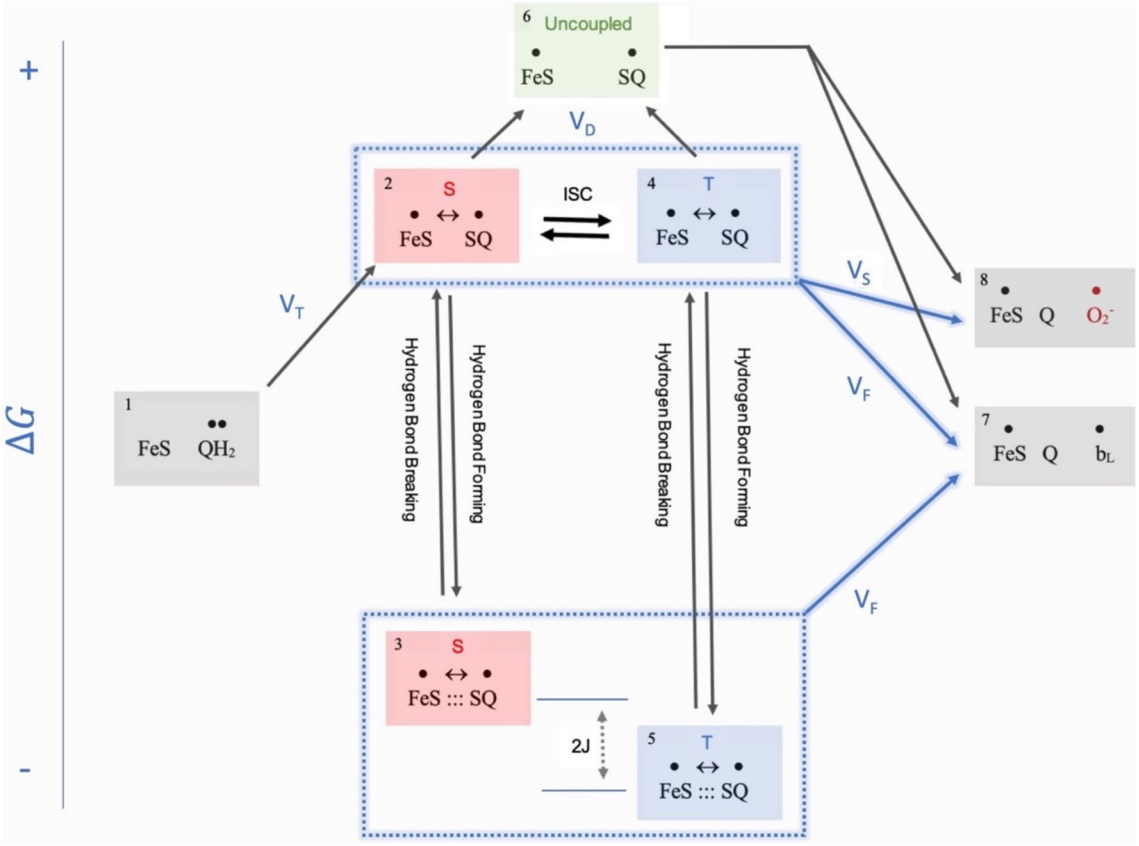

Fig. 15. A simplified schematic of the stages of electron transfer in the Q_O site of Complex III. Each box represents an electronic state. In contrast to states 2 and 4, the semiquinone in states 3 and 5 are attached to histidine of Rieske cluster which leads to large exchange value for the radical pair.

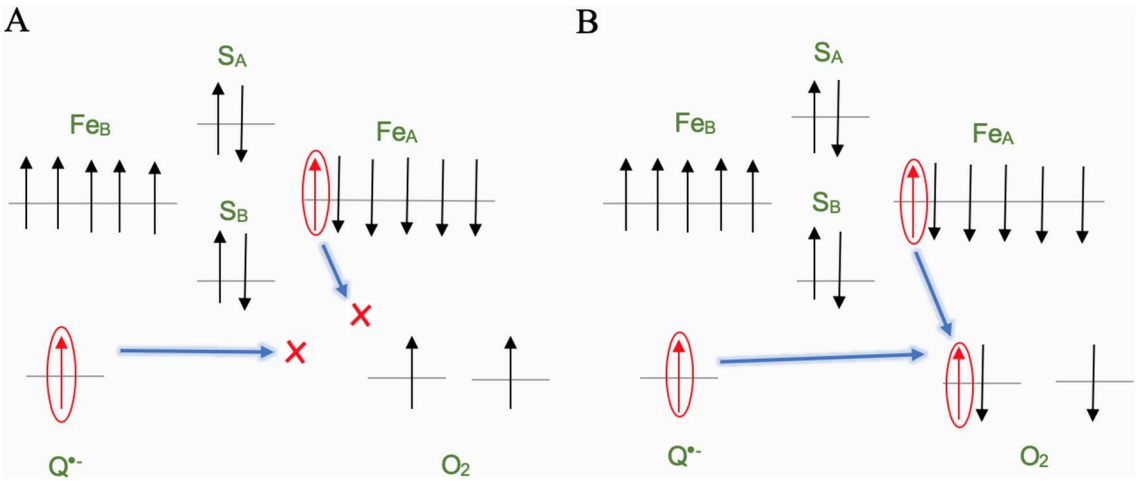

Fig. 16. Transfer of electron to the Oxygen molecule in the triplet state. In contrast to right section (**B**), a spin forbidden condition prevents the transfer of electron from either species of the Semiquinone/Iron-Sulfur radical pair to the oxygen molecule when electron spins aligned in the same direction (**A**).

agree that further investigations into the potential adverse effects of such fields, particularly regarding ROS-induced damage and their impact on the physiology of normal cells, are warranted.

We suggest an alternative method to influence the singlet–triplet interconversion rate without the need for high-intensity magnetic field used in the current study, thereby potentially avoiding any unknown adverse health effects. As an example, instead of applying an oscillatory 125 mT magnetic field in the range of a few Hertz

(ELF), a 3500 MHz magnetic field—corresponding to the J value calculated by Sarewicz et al. for the energy gap between singlet and triplet species in our suggested scheme—could be modulated within the ELF range to potentially resonate with both the interconversion frequency and RIRR frequency at two different timescales. The former resonance effect would allow for the use of magnetic fields with intensities several orders of magnitude lower than those used in the current study, possibly in the microtesla range. The effect of such therapeutically relevant field intensities can be still amplified within the framework of our model and warrant investigation in future studies. The effects of applying such radiofrequencies on ROS equilibrium have been observed previously in human cells, supporting the feasibility of the proposed resonance mechanism[68]. Particularly, the radical pairs formed via Fe-S cluster reduction in mitochondrial complex I are suggested as a potential site of this resonance for the applied frequencies[69].

Also, a more extensive investigation of ROS dynamics and their role in our model is suggested for future studies. The use of ROS suppressors, particularly mitochondrial superoxide inhibitors such as MitoTEMPO, could further elucidate the role of ROS dynamics by potentially mitigating the magnetic field-induced effects. Additionally, employing a more comprehensive profile of ROS probes, such as MitoSOX Red and Dihydroethidium (DHE) for superoxide detection, along with CellROX Orange and MitoPY1 for peroxide detection, could provide a more detailed understanding of the role of these species within the current proposed scheme.

Conclusion

Our study proposed a quantum biological mechanism for the effect of varying small magnetic fields on cancer cells. The frequency dependent effect of magnetic field is here postulated to be the result of interaction of alternating field with the intrinsically oscillatory system of coupled mitochondria via a novel radical pair phenomenon.

Here the site of action of the field is suggested to be the semiquinone/FeS radical pair in Complex III of ETC. A magnetic field of the order of few hundreds of millitesla is predicted to populate the triplet state of the radical pair whose electron transfer onto oxygen molecule is restricted by a spin forbidden reaction in half of the cases. This leads to a mild decrease in superoxide production in the presence of a such magnetic field. An oscillatory field can amplify such an effect via a resonance phenomenon in a network of coupled mitochondria in many cell lines. This substantial change in ROS balance can potentially cause physiological effect in the cells, including apoptosis. Our simulations show the mentioned effect can be manifested in two resonance modes: Either triggering the oscillation in network or synchronizing the out of phase oscillatory mitochondria. Our experimental results confirm the suggested model which can explain the previous observations for the first time. The hypothesis was validated by the observation of the synchronization when cells were exposed to sudden UV irradiation.

Moreover, we observed a frequency-dependent variation of the ROS concentration and mitochondrial membrane potential under the effect of oscillatory magnetic field in frequencies and intensities suggested by our model.

Further in vitro investigation with higher resolution of microscopy and more extensive profile of magnetic field frequencies and intensities can shed light on the detailed components of the involved mechanism.

Data availability

The datasets generated during fluorescent microscopy and numerical simulations are available from the corresponding author upon request.

Code availability

The code is accessible through the following doi on the Zenodo repository: https://doi.org/10.5281/zenodo.10902985.

Received: 1 September 2024; Accepted: 17 January 2025
Published online: 23 January 2025

References

1. Blackman, C. F. et al. Induction of calcium-ion efflux from brain tissue by radio-frequency radiation: Effects of modulation frequency and field strength. *Radio Sci.* **14**(6S), 93–98 (1979).
2. Goodman, R., Bassett, C. A. & Henderson, A. S. Pulsing electromagnetic fields induce cellular transcription. *Science* **220**(4603), 1283–1285 (1983).
3. Reiter, R. J. Melatonin in the context of the reported bioeffects of environmental electromagnetic fields. *Bioelectrochem. Bioenerg.* **47**(1), 135–142 (1998).
4. Adair, R. K. Constraints on biological effects of weak extremely-low-frequency electromagnetic fields. *Phys. Rev. A* **43**(2), 1039 (1991).
5. Binhi, V. N. & Rubin, A. B. Magnetobiology: the kT paradox and possible solutions. *Electromagn. Biol. Med.* **26**(1), 45–62 (2007).
6. Hoff, A. J., Rademaker, H., Van Grondelle, R. & Duysens, L. N. M. On the magnetic field dependence of the yield of the triplet state in reaction centers of photosynthetic bacteria. *Biochim. Biophys. Acta (BBA)-Bioenerg.* **460**(3), 547–554 (1977).
7. Blankenship, R. E., Schaafsma, T. J. & Parson, W. W. Magnetic field effects on radical pair intermediates in bacterial photosynthesis. *Biochim. Biophys. Acta (BBA)-Bioenerg.* **461**(2), 297–305 (1977).
8. Mims, D., Herpich, J., Lukzen, N. N., Steiner, U. E. & Lambert, C. Readout of spin quantum beats in a charge-separated radical pair by pump-push spectroscopy. *Science* **374**(6574), 1470–1474 (2021).
9. Zadeh-Haghighi, H. & Simon, C. Magnetic field effects in biology from the perspective of the radical pair mechanism. *J. R. Soc. Interface* **19**(193), 20220325 (2022).
10. Ritz, T., Thalau, P., Phillips, J. B., Wiltschko, R. & Wiltschko, W. Resonance effects indicate a radical-pair mechanism for avian magnetic compass. *Nature* **429**(6988), 177 (2004).

11. Wiltschko, W. & Wiltschko, R. Magnetic compass of European robins. *Science* **176**(4030), 62–64 (1972).
12. Santini, M. T., Ferrante, A., Rainaldi, G., Indovina, P. & Indovina, P. L. Extremely low frequency (ELF) magnetic fields and apoptosis: a review. *Int. J. Radiat. Biol.* **81**(1), 1–11 (2005).
13. Mansourian, M., Marateb, H. R. & Vaseghi, G. The effect of extremely low-frequency magnetic field (50–60 Hz) exposure on spontaneous apoptosis: the results of a meta-analysis. *Adv. Biomed. Res.* **5**, 141 (2016).
14. Okano, H. Effects of static magnetic fields in biology: role of free radicals. *Front. Biosci.* **13**(16), 6106–6125 (2008).
15. Yakymenko, I. et al. Oxidative mechanisms of biological activity of low-intensity radiofrequency radiation. *Electromagn. Biol. Med.* **35**(2), 186–202 (2016).
16. Mattsson, M.-O. & Simkó, M. Grouping of experimental conditions as an approach to evaluate effects of extremely low-frequency magnetic fields on oxidative response in in vitro studies. *Front. Public Health* **2**, 132 (2014).
17. Höytö, A., Herrala, M., Luukkonen, J., Juutilainen, J. & Naarala, J. Cellular detection of 50 Hz magnetic fields and weak blue light: effects on superoxide levels and genotoxicity. *Int. J. Radiat. Biol.* **93**(6), 646–652 (2017).
18. Kinsey, L. J., Van Huizen, A. V. & Beane, W. S. Weak magnetic fields modulate superoxide to control planarian regeneration. *Front. Phys.* **10**, 1356 (2023).
19. Brand, M. D. The sites and topology of mitochondrial superoxide production. *Exp. Gerontol.* **45**(7–8), 466–472 (2010).
20. Thannickal, V. J. & Fanburg, B. L. Reactive oxygen species in cell signaling. *Am. J. Physiol. Cell. Mol. Physiol.* **279**(6), L1005–L1028 (2000).
21. Toda, T. et al. Extremely low-frequency pulses of faint magnetic field induce mitophagy to rejuvenate mitochondria. *Commun. Biol.* **5**(1), 453 (2022).
22. Houston, B. J., Nixon, B., King, B. V., Aitken, R. J. & De Iuliis, G. N. Probing the origins of 1,800 MHz radio frequency electromagnetic radiation induced damage in mouse immortalized germ cells and spermatozoa in vitro. *Front. Public Health* **6**, 270 (2018).
23. Yap, J. L. Y. et al. Ambient and supplemental magnetic fields promote myogenesis via a TRPC1-mitochondrial axis: evidence of a magnetic mitohormetic mechanism. *FASEB J.* **33**(11), 12853 (2019).
24. Sarewicz, M., Dutka, M., Pintscher, S. & Osyczka, A. Triplet state of the semiquinone–Rieske cluster as an intermediate of electronic bifurcation catalyzed by cytochrome bc 1. *Biochemistry* **52**(37), 6388–6395 (2013).
25. Cape, J. L., Bowman, M. K. & Kramer, D. M. A semiquinone intermediate generated at the Qo site of the cytochrome bc1 complex: importance for the Q-cycle and superoxide production. *Proc. Natl. Acad. Sci.* **104**(19), 7887–7892 (2007).
26. Sarewicz, M. et al. Metastable radical state, nonreactive with oxygen, is inherent to catalysis by respiratory and photosynthetic cytochromes bc1/b6f. *Proc. Natl. Acad. Sci.* **114**(6), 1323–1328 (2017).
27. Walleczek, J. Magnetokinetic effects on radical pairs: A paradigm for magnetic field interactions with biological systems at lower than thermal energy. *Adv. Chem. Ser.* **250**, 395–422 (1995).
28. Eichwald, C. & Walleczek, J. Model for magnetic field effects on radical pair recombination in enzyme kinetics. *Biophys. J.* **71**(2), 623–631 (1996).
29. Kattnig, D. R. et al. Chemical amplification of magnetic field effects relevant to avian magnetoreception. *Nat. Chem.* **8**(4), 384 (2016).
30. Player, T. C., Baxter, E. D. A., Allatt, S. & Hore, P. J. Amplification of weak magnetic field effects on oscillating reactions. *Sci. Rep.* **11**(1), 9615 (2021).
31. Krylov, V. V. & Osipova, E. A. Molecular biological effects of weak low-frequency magnetic fields: frequency-amplitude efficiency windows and possible mechanisms. *Int. J. Mol. Sci.* **24**(13), 10989 (2023).
32. Belyaev, I. Y. & Alipov, E. D. Frequency-dependent effects of ELF magnetic field on chromatin conformation in *Escherichia coli* cells and human lymphocytes. *Biochim. Biophys. Acta (BBA)-Gen. Subj.* **1526**(3), 269–276 (2001).
33. Sarimov, R., Markova, E., Johansson, F., Jenssen, D. & Belyaev, I. Exposure to ELF magnetic field tuned to Zn inhibits growth of cancer cells. *Bioelectromagn. J. Bioelectromagn. Soc. Soc. Phys. Regul. Biol. Med. Eur. Bioelectromagn. Assoc.* **26**(8), 631–638 (2005).
34. Bauréus Koch, C. L. M., Sommarin, M., Persson, B. R. R., Salford, L. G. & Eberhardt, J. L. Interaction between weak low frequency magnetic fields and cell membranes. *Bioelectromagn. J. Bioelectromagn. Soc. Soc. Phys. Regul. Biol. Med. Eur. Bioelectromagn. Assoc.* **24**(6), 395–402 (2003).
35. Prato, F. S., Carson, J. J. L., Ossenkopp, K. & Kavaliers, M. Possible mechanisms by which extremely low frequency magnetic fields affect opioid function. *FASEB J.* **9**(9), 807–814 (1995).
36. Nezamtaheri, M. S., Goliaei, B., Shariatpanahi, S. P. & Ansari, A. M. Differential biological responses of adherent and non-adherent (cancer and non-cancerous) cells to variable extremely low frequency magnetic fields. *Sci. Rep.* **12**(1), 14225 (2022).
37. Henbest, K. B., Kukura, P., Rodgers, C. T., Hore, P. J. & Timmel, C. R. Radio frequency magnetic field effects on a radical recombination reaction: a diagnostic test for the radical pair mechanism. *J. Am. Chem. Soc.* **126**(26), 8102–8103 (2004).
38. Zorov, D. B., Filburn, C. R., Klotz, L.-O., Zweier, J. L. & Sollott, S. J. Reactive oxygen species (Ros-Induced) Ros release: a new phenomenon accompanying induction of the mitochondrial permeability transition in cardiac myocytes. *J. Exp. Med.* **192**(7), 1001–1014 (2000).
39. Zorov, D. B., Juhaszova, M. & Sollott, S. J. Mitochondrial ROS-induced ROS release: an update and review. *Biochim. Biophys. Acta (BBA)-Bioenerg.* **1757**(5–6), 509–517 (2006).
40. Aon, M. A., Cortassa, S., Marbán, E. & O'Rourke, B. Synchronized whole cell oscillations in mitochondrial metabolism triggered by a local release of reactive oxygen species in cardiac myocytes. *J. Biol. Chem.* **278**(45), 44735–44744 (2003).
41. Cortassa, S., Aon, M. A., Winslow, R. L. & O'Rourke, B. A mitochondrial oscillator dependent on reactive oxygen species. *Biophys. J.* **87**(3), 2060–2073 (2004).
42. Wang, W. et al. Superoxide flashes in single mitochondria. *Cell* **134**(2), 279–290 (2008).
43. Kuznetsov, A. V., Javadov, S., Saks, V., Margreiter, R. & Grimm, M. Synchronism in mitochondrial ROS flashes, membrane depolarization and calcium sparks in human carcinoma cells. *Biochim. Biophys. Acta (BBA)-Bioenerg.* **1858**(6), 418–431 (2017).
44. Novikova, I. N., Potapova, E. V., Dremin, V. V., Dunaev, A. V. & Abramov, A. Y. Laser-induced singlet oxygen selectively triggers oscillatory mitochondrial permeability transition and apoptosis in melanoma cell lines. *Life Sci.* **304**, 120720 (2022).
45. Yang, L., Korge, P., Weiss, J. N. & Qu, Z. Mitochondrial oscillations and waves in cardiac myocytes: insights from computational models. *Biophys. J.* **98**(8), 1428–1438 (2010).
46. De Jager, T. L., Cockrell, A. E. & Du Plessis, S. S. Ultraviolet light induced generation of reactive oxygen species. *Ultrav. Light Hum. Heal. Dis. Environ.*, 15–23 (2017).
47. Aykin-Burns, N., Ahmad, I. M., Zhu, Y., Oberley, L. W. & Spitz, D. R. Increased levels of superoxide and H_2O_2 mediate the differential susceptibility of cancer cells versus normal cells to glucose deprivation. *Biochem. J.* **418**(1), 29–37 (2009).
48. Hüser, J., Rechenmacher, C. E. & Blatter, L. A. Imaging the permeability pore transition in single mitochondria. *Biophys. J.* **74**(4), 2129–2137 (1998).
49. Feng, B. et al. Exposure to a 50-Hz magnetic field induced mitochondrial permeability transition through the ROS/GSK-3β signaling pathway. *Int. J. Radiat. Biol.* **92**(3), 148–155 (2016).
50. Chen, L. et al. Positive feedback loop between mitochondrial fission and Notch signaling promotes survivin-mediated survival of TNBC cells. *Cell Death Dis.* **9**(11), 1050 (2018).
51. Tomková, V., Sandoval-Acuña, C., Torrealba, N. & Truksa, J. Mitochondrial fragmentation, elevated mitochondrial superoxide and respiratory supercomplexes disassembly is connected with the tamoxifen-resistant phenotype of breast cancer cells. *Free Radic. Biol. Med.* **143**, 510–521 (2019).

52. Wang, S.-F., Tseng, L.-M. & Lee, H.-C. Role of mitochondrial alterations in human cancer progression and cancer immunity. *J. Biomed. Sci.* **30**(1), 61 (2023).
53. Sharpe, M. A., Baskin, D. S., Pichumani, K., Ijare, O. B. & Helekar, S. A. Rotating magnetic fields inhibit mitochondrial respiration, promote oxidative stress and produce loss of mitochondrial integrity in cancer cells. *Front. Oncol.* **11**, 768758 (2021).
54. Kalyanaraman, B. et al. Measuring reactive oxygen and nitrogen species with fluorescent probes: challenges and limitations. *Free Radic. Biol. Med.* **52**(1), 1–6 (2012).
55. Afzal, M. et al. Method to overcome photoreaction, a serious drawback to the use of dichlorofluorescin in evaluation of reactive oxygen species. *Biochem. Biophys. Res. Commun.* **304**(4), 619–624 (2003).
56. Gray, B. & Carmichael, A. J. Kinetics of superoxide scavenging by dismutase enzymes and manganese mimics determined by electron spin resonance. *Biochem. J.* **281**(3), 795–802 (1992).
57. Lin, M., Liu, T., Zheng, Y. & Ma, X. Dynamic light scattering microscopy sensing mitochondria dynamics for label-free detection of triple-negative breast cancer enhanced by deep learning. *Biomed. Opt. Express* **14**(10), 5048–5059 (2023).
58. Usselman, R. J., Hill, I., Singel, D. J. & Martino, C. F. Spin biochemistry modulates reactive oxygen species (ROS) production by radio frequency magnetic fields. *PLoS One* **9**(3), e93065 (2014).
59. Usselman, R. J. et al. The quantum biology of reactive oxygen species partitioning impacts cellular bioenergetics. *Sci. Rep.* **6**(1), 38543 (2016).
60. Zadeh-Haghighi, H. & Simon, C. Radical pairs and superoxide amplification can explain magnetic field effects on planarian regeneration. arXiv Prepr. arXiv:2312.06597 (2023).
61. Karogodina, T. Y., Dranov, I. G., Sergeeva, S. V., Stass, D. V. & Steiner, U. E. Kinetic magnetic-field effect involving the small biologically relevant inorganic radicals NO and O_2^{-}. *ChemPhysChem* **12**(9), 1714–1728 (2011).
62. Buettner, G. R. Superoxide dismutase in redox biology: the roles of superoxide and hydrogen peroxide. *Anti-Cancer Agents Med. Chem. (Formerly Curr. Med. Chem. Agents)* **11**(4), 341–346 (2011).
63. Hagras, M. A., Hayashi, T. & Stuchebrukhov, A. A. Quantum calculations of electron tunneling in respiratory complex III. *J. Phys. Chem. B* **119**(46), 14637–14651 (2015).
64. Hung, S.-C. et al. Electron spin–lattice relaxation measurement of the 3Fe-4S (S-3) cluster in succinate: ubiquinone reductase from *Paracoccus denitrificans*. A detailed analysis based on a dipole–dipole interaction model. *J. Phys. Chem. A* **104**(19), 4402–4412 (2000).
65. Yamashita, K. & Saito, M. Effects of middle-level static magnetic field on metabolic activity of mitochondria. *Electr. Eng. Japan* **137**(1), 36–41 (2001).
66. Salo, A. B., Husen, P. & Solov'yov, I. A. Charge transfer at the Qo-site of the cytochrome bc 1 complex leads to superoxide production. *J. Phys. Chem. B* **121**(8), 1771–1782 (2016).
67. I. C. on N.-I. R. Protection. Guidelines on limits of exposure to static magnetic fields. *Health Phys.* **96**(4), 504–514 (2009).
68. Chow, S.-C. et al. External RF-EMF alters cell number and ROS balance possibly via the regulation of NADPH metabolism and apoptosis. *Front. Public Health* **12**, 1425023 (2024).
69. Gurhan, H. & Barnes, F. Impact of weak radiofrequency and static magnetic fields on key signaling molecules, intracellular pH, membrane potential, and cell growth in HT-1080 fibrosarcoma cells. *Sci. Rep.* **13**(1), 14223 (2023).

Author contributions

Amirali Zandieh: Conceptualization, Simulation's data collection, Data analysis, and Manuscript draft preparation Seyed Peyman Shariatpanahi: Project Supervision, Conceptualization, Experimental Design, and Manuscript Revision Amir Abas Ravassipour: Experimental Design, Experimental data collection, and Data Analysis Javad Azadipour: Experimental data collection, Data Analysis, and Manuscript draft preparation Maryam Sadat Nezamtaheri: Experimental data collection Zahra Habibi-Kelishomi: Experimental data collection Mojtaba Ghanizadeh: Conceptualization Ali Same: Data analysis Keivan Majidzadeh-A: Supplying experimental equipment and Analysis Validation Amir Taheri: Manuscript Revision and Analysis Validation Alireza Madjid Ansari: Manuscript Revision and Analysis Validation Mohammad Amin Javidi: Manuscript Revision and Analysis Validation Mohammad Mehdi Pirnia: Simulation's data collection Bahram Goliaei: Project administration, Supplying experimental equipment, Project Supervision All authors reviewed the manuscript.

Declarations

Competing interests

The authors declare no competing interests.

Additional information

Supplementary Information The online version contains supplementary material available at https://doi.org/10.1038/s41598-025-87235-w.

Correspondence and requests for materials should be addressed to S.P.S. or B.G.